The influence of acrylate triblock copolymer embedded in matrix on composite structures' responses to low-velocity impacts

Sébastien Denneulin [a,*], Philippe Viot [a], Frédéric Leonardi [b], Jean-Luc Lataillade [a]

[a] Arts et Métiers Paristech, I2M, UMR CNRS 5295, Esplanade des Arts et Métiers, F-33405 Talence, France
[b] IPREM–EPCP–CNRS UMR 5254, Hélioparc Pau Pyrénées, 2, Avenue du Président Angot, F-64053 Pau, France

Keywords:
Composite
Low-velocity impact
Dynamic test
Drop tower
Nanoparticle

A B S T R A C T

In passive safety structures the use of composite materials has increased significantly recently due to their low specific mass and high energy absorption capacities. The purpose of this experimental study is to describe the macroscopic behaviors of different Kevlar woven composite materials with different kinds of matrix (pure and with acrylate based block copolymer additives: Nanostrength®) under low-velocity impact. Tests were performed with a drop weight tower on square plates ($100 \times 100\,mm^2$) clamped by means of a circular fixture. Images were recorded during impact by a high-speed video camera fixed underneath the plate. It was found that Kevlar epoxy composite material with Nanostrength M52N has the best resistance to perforation.

The second purpose is to study the influence of physicochemical parameters (fibers ratio, percentage of M52N, micro-porosity) on the behavior of the selected composite material. Based on correlation between pictures, displacement, and loading histories, two criteria are defined to quantify the energy absorption capability of the composite material just before the fibers' failure and after perforation of the plate. A high-fiber weight improves performance regarding criteria and also improves the efficiency of the block copolymer present in the epoxy matrix.

1. Introduction

In passive safety applications such as helmets and knee pads structures are used to protect a person from impact by absorbing or dissipating the impact kinetic energy, while keeping the acceleration supported by the person below a non-dangerous value threshold. During the shock, passive safety structures must also avoid any contact between the projectile and the impacted body, in order to reduce the severity of injury. For each particular application, specific materials and geometric structure have to be chosen. Helmet structures are then designed (whether they are used for sports, motorcyclists, or aeronautic applications) to improve the capacity of the structure to absorb kinetic energy of the impact, to limit perforation of the structure, and to avoid any contact between sharp projectiles and the user's head [1,2]. All the components of the helmet structure, more particularly the outer shell and inner foam part, must be defined to reach the objectives imposed by the standards. Polymeric foams are widely used in helmet structures to dissipate a significant part of the impact energy through their irreversible deformation [3]. The outer shell must be designed with the greatest attention since this structure has several essential roles during impact: The shell must resist perforation by the projectile (its main role) and dissipate part of the energy through its plastic deformation, failure. Moreover, it must spread the dynamic loading across the largest area of the inner foam (even in the case of a sharp projectile) to induce an irreversible deformation (synonym with dissipation of energy) on the largest volume of foam.

The use of composite materials for helmet shells has increased significantly recently because of their low specific mass, stiffness, and high energy absorption capacities. Polymer such as polypropylene and polyethylene are already used for the cheap helmets or for light cyclist ones, whereas glass-fiber composites are used for basic helmets, and aramid fibers or carbon fibers are reserved for high-technology helmets. For this project, a Kevlar fiber fabric composite was chosen for the shell of an helmet because of its low-density, high ultimate strain, and ultimate strain even at high rates of deformation [4]. The study's objective was to improve the performance of the shell (taking into account perforation criteria) by changing the properties of the matrix.

Epoxy matrix used in composite material is brittle and shock sensitive, so, to toughen the matrix epoxy, a common approach is including a softer phase (core shell particles) that does not react in the matrix. The difficulty with the core shell particles is achieving

* Corresponding author.
E-mail addresses: sebastien.denneulin@ensam.eu (S. Denneulin), philippe.viot@ensam.eu (P. Viot).

a uniform dispersion because of crosslinks in the epoxy resin. Due to this difficulty, they are used at high concentrations and thus scarify strength and rigidity. By using nano-reinforcement, it is expected that a low concentration brings significant improvements without scarifying other properties. Matrix toughened by nano-reinforcement have been demonstrated already [5–7], but few papers have been published on the mechanical behavior of multi-scale composites [8,9].

From this context, the objective of this research is to evaluate the response of composites based on Kevlar fiber with different types of matrix, including various block copolymers. The effect of these nanocharges on the composites under low velocity impact is firstly investigated at the macroscopic and mesoscopic scales. This paper is then divided into three parts. After presenting the characteristics of used composite materials and the choice of drop weight test conditions, macroscopic responses of the composite plates are discussed and the damage caused by the perforation is analyzed at the microstructural scale. Finally, influences of physico-chemical parameters, such as fiber weight ratio and microporosities are discussed.

2. Material and experimental tests

2.1. Matrix

Epoxy matrix is brittle and not very much shock resistant because of its low-strain energy release rate (G_{1c} = 180 J m^{-2}). The strain energy release rate is increased up by a factor 10 by the addition of block copolymers M52N in epoxy matrix [5]. Nanostrength block copolymers are efficient with a low concentration because when they are dissolved in the diglycidyl ether of bisphenol A (DGEBA) resin, they self-assemble into nanostructures, which ensures good dispersion. Block copolymers low concentration prevents epoxy matrix from decreasing in strength and rigidity. Moreover, the small size of block copolymers allows repartition even within small inter-fiber spacing on composite material.

2.1.1. Epoxy resins

The thermoset epoxy precursor DGEBA is a low viscosity a liquid epoxy supplied by Axson Technologies. The hardener was used in the ratio 0.345 (w/w) (34.5 g of hardener for 100 g of precursor).

2.1.2. Nanostrength®

Nanostrength, provided us by ARKEMA (GRL, France), are symmetric MAM copolymers with two poly(methyl methacrylate) blocks surrounding a center block of poly(butyl acrylate). PMMA blocks have a strong affinity with DGEBA matrix, which allows for a good dissolution in it. But, Serrano et al. [10] have shown that making a random copolymers of methyl methacrylate (MMA) and N, N-dimethylacrylamide (DMA) can be used as a miscible block for the DGEBA system to enhanced the dispersion of this block in the epoxy matrix, and give better property with polar hardener, which is the case with our matrix. Then nanostructuration is induced by strong repulsions between the side and middle blocks governed by thermodynamics and is thus independent of processing conditions. Various copolymers are commercially available depending on their molecular weight and PMMA/PBA ratio and are suitable depending on the hardener. A complete physico-chemical characterization of the three block copolymers has been performed using Gel Permeation Chromatography in THF solvent and Nuclear Magnetic Resonance in order to derived important parameters as we can see below in Table 1.

After preliminary tests on three Kevlar composites formulations (M22, M42, and M52N, Fig. 2) the M52N was chosen to toughen our epoxy system because of its good performance regarding perforation resistance (Fig. 9).

2.1.3. Epoxy resin filled in Nanostrength M52N

A variable amount of M52N (5–15 g) was added to 100 g of precursor to demonstrate the effect of this filler on the response of the composite structure. The different matrix compositions are summarized in the Fig. 1.

To check the self-assembling process of the triblocks copolymer, Nanostrength, some nano pictures were taken with the Transmission Electronic Microscopy (TEM) on 60 nm slices. The first three pictures (Fig. 2a) shows the morphology of different nanoparticles. The M22 and M42 seem to have bigger particles, which are less well distributed than the M52N particles. Fig. 2b seems to confirm the homogeneous reparation of M52N block copolymers for the three used concentrations.

2.2. Fabrics

A Kevlar fiber fabric composite was chosen for this study because of its very high tensile toughness (σ_r = 3.4 Gpa, ε_r = 3.5%) [11]. A large affected zone is expected to dissipate the shock energy as much as possible. Preliminary tests have shown that a plain-woven fabric has good resistance to impact out of the plane [12].

Kevlar® 129 (Saatilarâ Style 802; taffeta 190 g/m^2; thickness: 260 μm) was used for all thermoset composite preparations. The

Table 1
Physico-chemical characterization of the three block copolymers used as nanofiller.

Block copolymer	Molecular Weight Distribution parameters obtained by GPC in THF				Composition (% molar) derived from ^{1}H NMR		
	Mw (kg/mol)	Mn (kg/mol)	Ip	dn/dc (mL/g)	PBuA	PMMA	PDMA
M22	126	94	1.35	0.082	36	64	
M42	208	146	1.43	0.072	31	69	
M52N	147	95	1.54	0.071	45.6	43	11.4

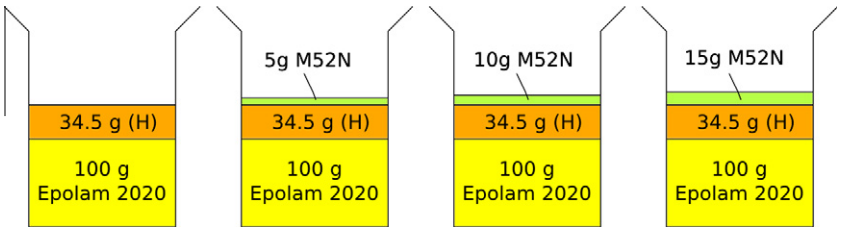

Fig. 1. Different matrix composition.

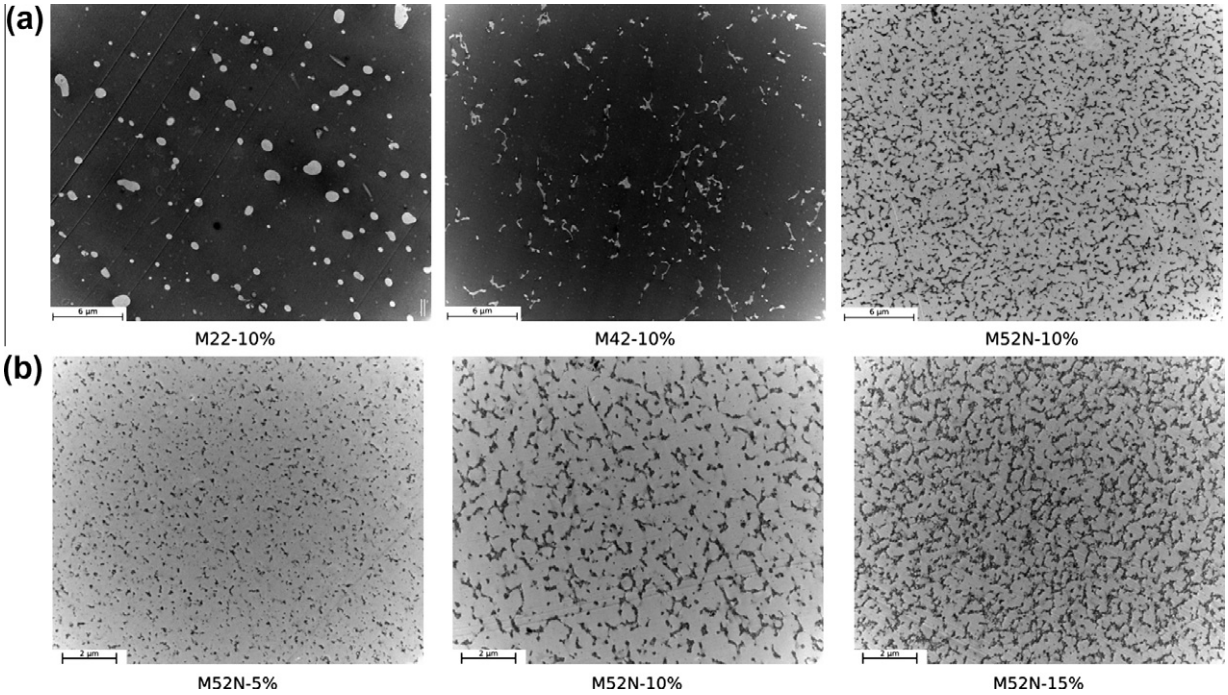

Fig. 2. (a) Different matrix composition (TEM observation). (b) Different percentage of Nanostrength M52N (TEM observation).

Table 2
Kevlar 129 properties.

Material	Fiber's trade name	Tensile strength (GPa)	Tensile modulus (GPa)	Strain to failure (%)	Density (g m^3)
Aramid	Kevlar 129	3.4	99	3.3	1.45

fiber's mechanical properties are given in Table 2. The fiber's diameter is about 12 μm and was measured by microscopy.

2.3. Composite and sample preparation

2.3.1. Epoxy resins preparation

The addition of all block copolymer in the precursor is performed by mixing at 290 rpm at 90 °C during for 90 min. Then just before impregnation, the mixture is heated at 40 °C for 5 min for degassing.

2.3.2. Composite preparation

All thermoset epoxy composites were prepared in the same way. The Kevlar fabric was oven for 20 min at 80 °C before each layer of fabric was impregnated manually (with a brush) with a blend of epoxy precursor and hardener. Then, the three impregnated layers of fabrics (Kevlar®) were disposed with a 0° orientation between two sheets of paper in a press. A three-stage process was required to provide thermoset composites. The first stage was compression of the impregnated layers under 1.5 bars for 5 min. The second was a curing cycle at a temperature of 90 °C under the same pressure for 90 min. Finally, the composites were post-cured in an oven at 80 °C for 2 h. Fiber weight fractions of these composite materials have been determined by Thermo-Gravitation Analysis and are close to 65%. Material characteristics are summarized in Table 3.

For the study on the influence of the fiber weight ratio, the only protocol parameter that changes is the curing pressure.

2.4. Experimental device

Low-velocity impact tests aim are to generate on composite plate specimens damage equivalent to that observed on real helmet structure after an impact and to study the influence of physico-chemical parameters on composite behavior. For this purpose two series of tests were performed with different initial conditions.

For the first series of tests, the initial conditions (in terms of ranges of velocity and energy) and the boundary conditions of the impact tests on composite specimens have to be close to the conditions imposed on the helmet (regarding the standard recommendations [13]). Impact tests carried out with a drop weight tower on a previous generation of helmet (using a Kevlar/Epoxy shell) revealed matrix cracks, delamination, and fiber breakage at the impact point. Test conditions were chosen to highlight observed damage mechanisms and to highlight the effects of the co-polymer Nanostrength during specimen impact testing. These tests revealed that there was no perforation on the Epoxy-NS-3K plate, whereas there was perforation on the Epoxy-3K.

In a second series of tests, the impact energy was increased to perforate the composite plate, and systematically initiate all the damage mechanisms. In this part, the influence of physico-chemical parameters (fiber weight fraction, percentage of Nanostrength, and degassing effect) were studied.

Drop tower and gas canons can be used to test composite structures under impact [14], the final objective being to launch a projectile with either gravitational force (in the case of a drop tower) or with gas pressure in the case of the canon. These facilities were both available in the laboratory but the drop tower was selected for the range of impact velocities and for its instrumentation [15].

2.4.1. Drop tower and its instrumentation

The drop tower used for this study consists of two rectified columns attached to a metallic gantry (Fig. 3a and b). These two columns guide the falling carriage, on which different impactor geometries can be fixed. A winch with an electromagnet was used to lift the projectile (from 1 kg to 5 kg) to the desired impact height

Table 3
Composition and characterization of samples and composites prepared.

Sample	Composition	Surface density (g/m^2)	Thickness (mm)
Epoxy-3K	Epoxy, 3 layers of Kevlar®	930	0.8
Epoxy-NS-3K	Epoxy + 10% M52N, 3 layers of Kevlar®	920	0.8
Kevlar M52N 5%	Epoxy + 5% M52N, 3 layers of Kevlar®	976	0.8
Kevlar M52N 15%	Epoxy + 15% M52N, 3 layers of Kevlar®	1016	0.8

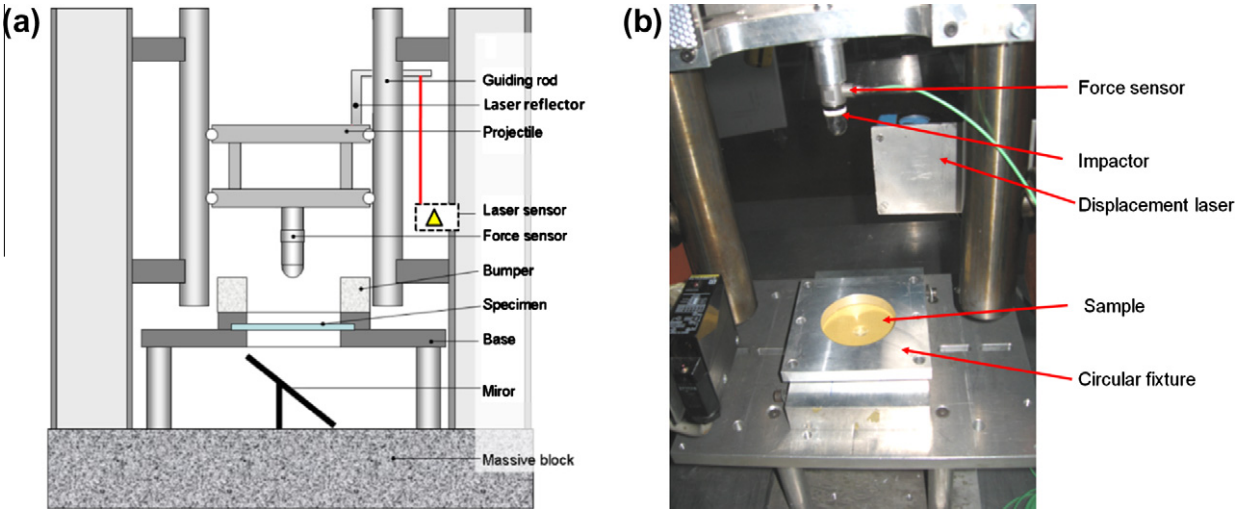

Fig. 3. Specimen mounting device.

(up to 2 m) in the function of the velocity required. During the test, the projectile is released by an electromagnet, freefalls, and strikes the structure. An anti-bouncing device is implemented to avoid a second shock, which could further damage the structure and prevent a post-mortem analysis of the damage and residual strain. This anti-bouncing device is particularly useful for further damage analysis.

A laser sensor (10 mm effective range) measures the impactor displacement during the fall, the impact phase, and the rebound. The experimental velocity can be obtained by a linear regression of the projectile displacement and compared to the theoretical velocity given by the formula $\sqrt{2gh}$, with g denoting the gravitational acceleration and h the drop height. By putting a piezoelectric force sensor (Bruel & Kjaer 8230 C-003 force transducer, force range of 5 kN) under the projectile, the force response of the structure during impact can be determined. The signals of both sensors are recorded by a PC card acquisition at a frequency of 30 kHz. These devices are supplemented by a Photron FASTCAM-APX RS high-speed video camera. This optical apparatus makes it possible to observe the lower face of the composite structure during the shock (a mirror was placed at 45° beneath the sample to reflect the image of the deformed sample) to better understand the test results. Displacement is also measured from a second high-speed video camera (Photron SA3), which tracks a grid stuck on the impactor.

2.4.2. Boundary conditions

During the test, the specimen was held with clamped edge conditions in a circular support 70 mm in diameter (Fig. 3). The plates were clamped by four screws with a torque of 20 Nm. Similar devices were used [12] to evaluate the response of composite laminates under drop test, using a circular fixture. Other works have been published on woven composites. Alcock et al. [11] used a similar mounting device to study the performance of recyclable all-polypropylene woven composites. Sevkat et al. [16] and Tita et al. [17] made a similar mounting device with respectively, a 76.2-mm and an 80-mm circular support to study impact performance of carbon, glass, and hybrid composites. Consequently, a circular fixture with clamped boundaries was chosen for this study.

The steel impactor has a hemispherical shape 16 mm of diameter to correspond to the ones imposed by aeronautic standards, but the shape was principally chosen to generate on composite plates damage such as matrix cracking, delamination, and fiber breakage. Ballere and Viot [15,18] had already used this kind of impactor to evaluate carbon epoxy structure response under low-velocity impact tests, and fiber breakage and delamination were detected in the composite structure. Furthermore, Mitrevski et al. [19] studied the effect of impactor shape on the impact response of composite laminates. Three impactor shapes, (hemispherical, ogival, and conical) have been used to impact woven carbon/epoxy laminates with initial impact energies of 4 and 6 joules. The hemispherical impactor produced the highest peak force, the shortest contact duration, and damage close to that observed on our structure.

2.4.3. Initial conditions

For the first tests, the velocity of the impactor is 3.13 ms^{-1}, with a mass of 1.77 kg. Its mass and drop height of 0.5 m were determined from iterative tests to obtain significant damage on the composite specimens.

For the second series of tests, the drop height was double (1 m) to enable the impactor to reach a velocity of 4.43 ms^{-1}; the impactor's mass was unchanged. With this velocity corresponding to 17.4 joules, perforation occurred for each composite plate. Impact conditions are summarized in the Table 4.

Preliminary tests were carried out and results highlight the good quality and reproducibility of the drop test apparatus.

Table 4
Impact conditions for the two series of tests.

Impact conditions	Drop height (m)	Velocities (ms^{-1})	Mass (kg)	Energy (J)	Impactor diameter (mm)	Clamping diameter (mm)
1	0.5	3.13	1.77	8.7	16	70
2	1	4.43	1.77	17.4	16	70

3. Results

3.1. Results on the macroscopic scale

3.1.1. Typical results

For each type of composite material, several specimens (3–6) were tested under the same conditions. The typical variations of displacement and force as a function of time measured by the force sensor and the video analysis are presented in Fig. 4.

The other camera was used to record pictures showing the deformation of the back face of the composite specimen during impact, and because the record of the film was triggered with the measurement of the displacement sensor, the force and displacement curves can be analyzed with a view of the sample deformation at the same instant.

The beginning of the test was defined when the force reached 50 N and the two curves were adjusted to consider this instant t_0 as the starting point of the impact.

For the displacement vs. time curve, we can notice:

- Before t_0, the displacement vs. time is parabolic since the impactor was just loaded by the gravitational force and the friction (assuming it to be constant) between the impactor and the two columns of the drop tower. This part of the curve was used to check the initial velocity of the impactor.
- Between t_0 and 10 ms, the velocity of the impactor decreases to tend to zero (i.e. the slope of the displacement curve decreases). The impactor is in contact with the sample, which imposes a reaction force.
- After 10 ms, the slope of the displacement curve changes and becomes positive showing the rebound of the impactor at the end of the test due to the elastic response of the deformed composite plate. In this case, the rebound is not significant (the curve slope is weak) since a significant perforation can be observed (Fig. 4e).

Four phases can be distinguished for the variation of force vs. time during the Epoxy-3K impact:

- The first phase corresponds to the elastic bending of the plate. After $t = 0$, the force increases progressively during less than 1 ms (corresponding to the delay to obtain a straight contact between impactor and samples). After this delay, the significant increase in the force history is due to the elastic response of the composite sheet. At t_1, the force reaches 1 kN.
- Within the interval $[t_1, t_2]$, the increase in the force signal is lower, revealing a first decrease in the rigidity of the sample due to damage initiation in the composite structure. These damages are mainly matrix cracking and are responsible for a small

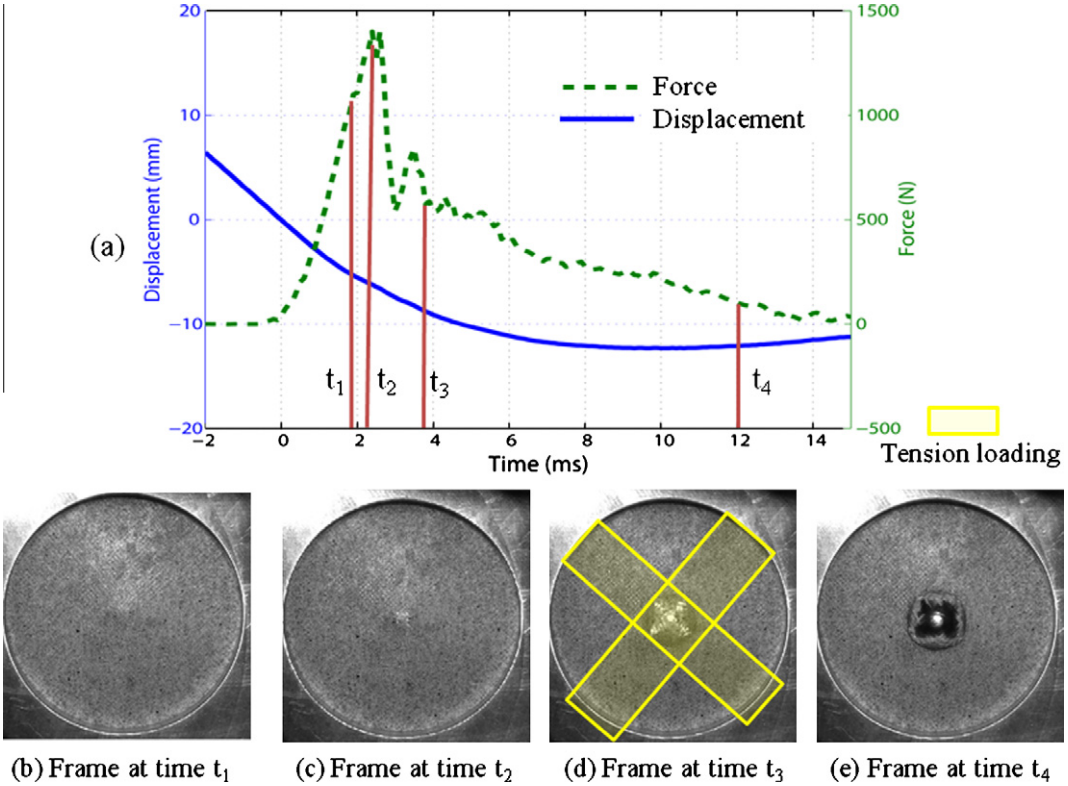

Fig. 4. Epoxy-3K composite plate. (a) Force and displacement curves. (b), (c), (d), and (e) show the underside of the plate at specific times.

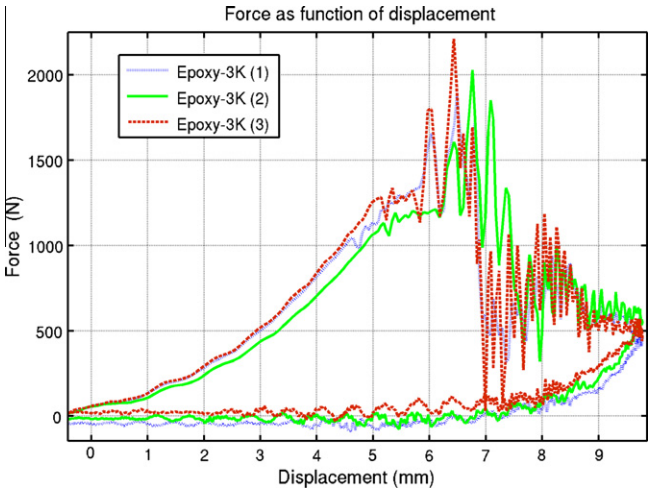

Fig. 5. Displacement vs. force curves during an impact on Epoxy-3K plates.

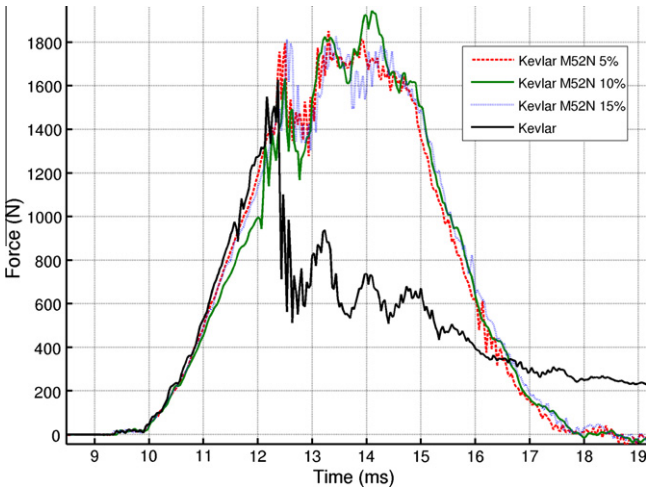

Fig. 6. Force vs. time curves during the impact test with impact conditions 1. One representative test for 0%, 5%, 10%, and 15% of M52N.

oscillation (that can be observed in Fig. 5 between 4.5 mm and 6.5 mm of displacement). At the instant t_2, the recorded picture reveals visible damage located at the impact point (the composite color underneath the impactor becomes white because of matrix cracking). The maximum force of 1.4 kN is reached at time t_2.

- Within the interval [t_2, t_3], the force decreases significantly because of the damage propagated in the structure. A complementary analysis of the post-impact structures (see Section 3.2) shows that fiber breakage was initiated during the impact of the Epoxy-3K composite plate. Fiber breakage is a brief phenomenon (the duration of the strong decrease in force is less than 1 ms) that induces a loss of rigidity and resistance in the composite structure. At t_3, the fiber breakage is clearly visible (see picture 4d). In fact, during the deformation, two main bands of composite were loaded in tension; these bands are oriented along the principal direction of the woven composite structure and the Kevlar fibers were dynamically loaded in tension. For a maximum force reached at time t_2, the local stress at the impact point overcame the fiber strength in tension, and fiber breakage was propagated. From this observation, the mean magnitude of strain rate can be evaluated. Indeed, if the failure strain is 3.5% and the time to breakage is about 3.8 ms, the mean strain rate is 9.2 s^{-1}. Due to a strong localization close to the impacted site, a higher strain rate is expected at the center. Several authors have found similar damage shape. Gustin et al. [20] performed similar impact tests on a Kevlar sandwiches and obtained similar damage on the composite sheet. Alcock et al. [11] performed drop tower tests on polypropylene composites and noticed the two tension bands were oriented in a cross in the middle of the impacted plate.
- After t_3, the last phase corresponds to the residual strength of the plate and the dry friction during the penetration of the impactor into the structure.

3.1.2. Behaviors dispersion

The measurements of force and displacement as a function of time made it possible to plot the force vs. displacement curve. For each kind of composite material tested, a weak dispersion of material behavior was revealed on these force/displacement curves: just the strong oscillations initiated during the fiber breakage are not reproducible. The veracity of this result is illustrated in Fig. 5 where the weak dispersion of the behavior of impacted Epoxy-3K plates can be noticed. Only a representative force/displacement curve for each kind of material is then presented to compare their behavior.

3.1.3. Influence of the M52N percentage

In order to choose the best percentage of M52N copolymer, three types of composite plate are tested. The first impact conditions are used and the contact force vs. time is presented in Fig. 6. A significant improvement is noticed, whatever the percentage of M52N is compared to the Epoxy-3K. However, damage is revealed on 10% of the M52N (Fig. 9) composite plate, which is much less severe than the others. Finally, the composite plate with 10% M52N has been chosen for all further investigations.

3.1.4. Comparison of the response of the impacted structures

A comparison of the behaviors of the composite material can be done from the force vs. displacement response (Fig. 7). A first conclusion can be directly made from Fig. 7; it is shown that the addition of copolymers significantly changes the composite behavior.

In the first phase of elastic bending the elastic stiffness is reduced by the addition of copolymers, which may be explained by the more compliant elastomeric phase. However, elastic limits, detected by the first oscillation on the curve due to matrix cracking, are increased about 40% in terms of force (1000–1400 N) and about 30% in terms of displacement (4.5–6.5 mm).

The second phase of damage propagation occurs until a maximum force of 1800 N for both composites. However, the third phase, which corresponds to fiber breakage and perforation, occurs only for the Epoxy-3K. No perforation and penetration is recorded for the Epoxy-NS-3K, whereas a fourth phase with high friction (600 N) is measured for the Expoxy-3K.

Finally, the analysis of the macroscopic response of the impacted Epoxy-NS-3K shows the effect of elastomeric nanoparticles on:

- a lower elastic stiffness, which may be explained by the more compliant elastomeric phase;
- a higher strength and an absence of brutal fall of rigidity (due to fiber breakage and perforation of the Epoxy-3K).

To conclude, concerning the comparison of the macroscopic responses of these materials, the energy dissipated by these different composites is quite similar (it corresponds to the large hysteresis loop area) but the phenomena involved in dissipating the impact energy are different. Fiber breakage imposed during the perfora-

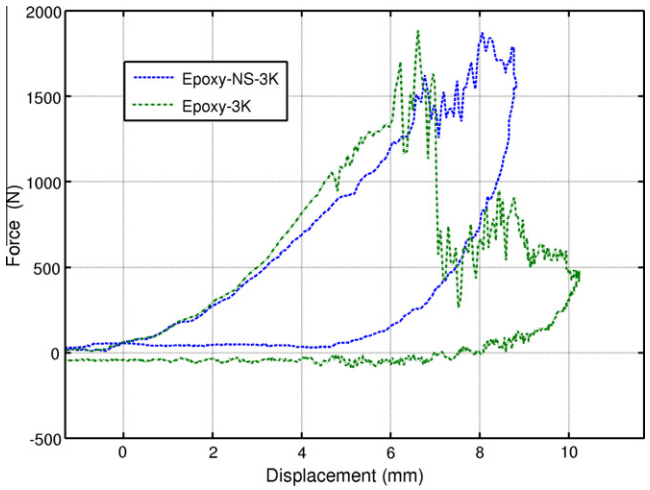

Fig. 7. Representative force vs. displacement behavior during impact on Epoxy-NS-3K and Epoxy-3K.

tion of Epoxy-3K is preponderant, whereas it is probably the matrix damage and delamination which involve energy dissipation in the case of Epoxy-NS-3K. These results were confirmed by a post-mortem analysis.

3.2. Post-mortem analysis

3.2.1. Observation at the macrostructure scale

An analysis of the force/displacement responses of the impact test on the composite materials made it possible make conclusions about fiber breakage and perforation of Epoxy-3K. The post-mortem observations of the impacted sheet confirmed these results deduced from macroscopic measurements. The Epoxy-3K plates were perforated by the projectile, whereas no relevant indentation can be noticed on Epoxy-NS-3K. Fig. 8 shows the state of damage that can be observed on the composite plates just after the impact test. The impact damage zones of the first two candidates (M22N and M42N) are presented and a perforation zone is clearly detected. On the Epoxy-3K plates, the damage is localized and fiber breakage can be easily detected:

- For Epoxy-3K, significant matrix cracks can be deduced from the white color of the epoxy resin. From the orientation of the fiber breakages (in a cross way) we can assume a tensile loading of the fiber in the 0° and 90° directions of the woven composite.
- It has been pointed out that the Epoxy-NS-3K response under impact was significantly different. Hence, after impact, the composite structure did not present (to the naked eye) any fiber breakage; it has been noticed just as a light permanent deformation.

From pictures of impacted plates (Fig. 9) obtained by transparency, two damage zones can be clearly seen. The first zone is close to the impact point and the second is localized in the vicinity of the circular fixture. The damage in the vicinity of the circular fixture is due to the bending moment, which depends mainly on the plate diameter. Here the boundary conditions are similar for each test so the damage due to the boundary condition is not considered in this study. The second zone, which corresponds to the impact site, exhibits two very different morphologies. For the Epoxy-3K, the picture obtained by transparency confirms the previous observation that the damage is localized in the indentation zone. This damage is mainly fiber failure in the center and matrix cracking in the vicinity of the impactor. For the Epoxy-3K-NS, the damage is much more concentrated along the fibers' direction (0° and 90° which formed this cross). The dimensions of the affected area are larger and principally due to matrix failure and the delamination zone.

These first remarks issued from observations on the samples just after the drop test were confirmed by post-mortem measurements on the plate section at the center of impact (Fig. 10). The two samples were embedded in a matrix and cut in a perpendicular section in the straight impact point in order to measure precisely the permanent deformations of the structure and to observe the damaged structure with an optical microscope.

The residual indentations were deduced from impactor displacements (Fig. 7, when the force gets back to zero), and they were 4.0 mm and 7.3 mm for the Epoxy-NS-3K and Epoxy-3K, respectively.

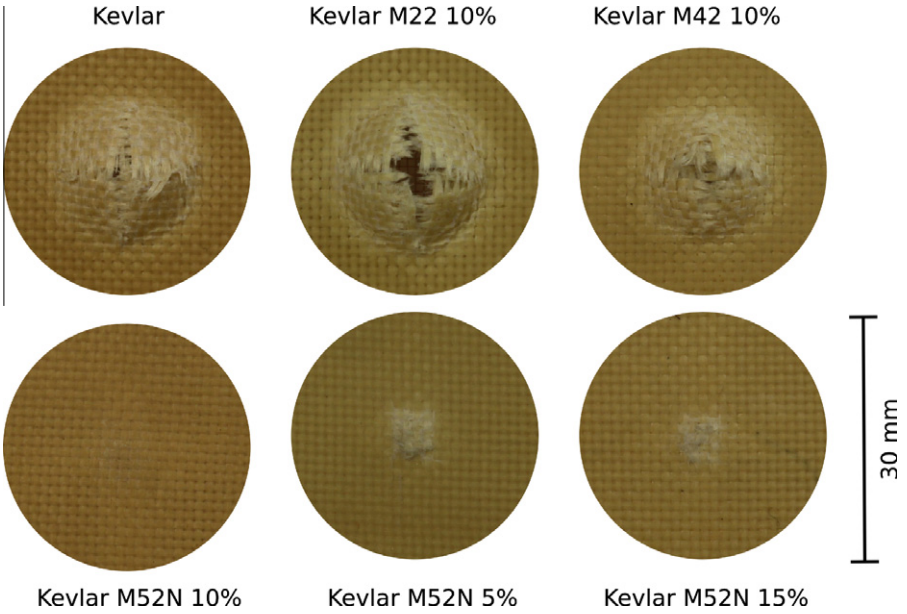

Fig. 8. Impact damage. The diameter is 30 mm ±0.1.

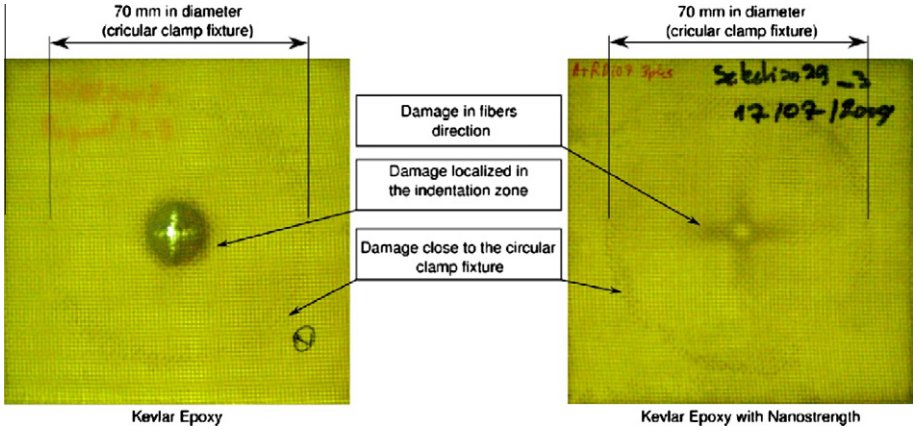

Fig. 9. Impact damage visualized by transparency with a lightbox.

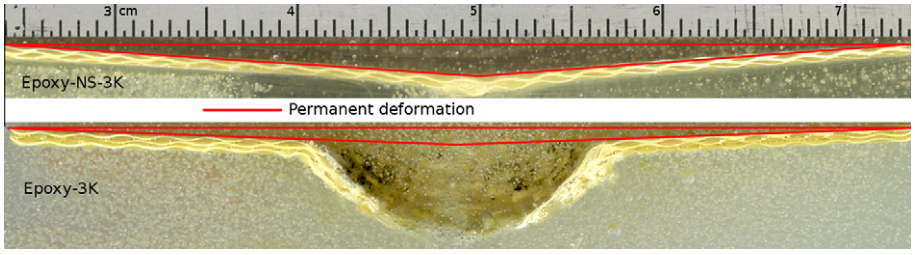

Fig. 10. Comparison between cross-sections of the impacted plate.

These results were confirmed by the permanent indentation measurements obtained on the cross-sections (Fig. 10), although smaller values were measured due to the viscoelastic character of the material. From these cross-section observations, it can be immediately deduced that the perforation is relevant for Epoxy-3K. Furthermore, the damage is localized close to the impact zone even if a residual deformation of the whole of the plate can be measured: the height of the cone of deformation of the Epoxy-3K samples is less than 1 mm, whereas the height of localized indentation is three times as important. In fact, a deep permanent indentation with a strong localization of deformation is a disadvantage for helmet application because impact energy is spread on a restricted zone of the inner foam structure.

For Epoxy-NS-3K, the deformation was spread on the whole of the composite plate; the height of the cone of deformation is less than 2 mm (which corresponds roughly to the impactor displacement measurement), and any localization of damage cannot be seen at this observation scale.

3.2.2. Observation at the microstructure scale

These cross sections were observed with an optical microscope to detect the different kind of damage mechanisms involved during impact.

3.2.2.1. Microscopic observation on Epoxy-3K. The damage to the Epoxy-3K microstructure was concentrated in the indentation zone; in the vicinity of this zone (Fig. 11) the structure of the three composite layers does not seem affected by the impact, and the geometry of the cross-sections of the composite yarns is not modified. The effect of the impact on the structure is particularly

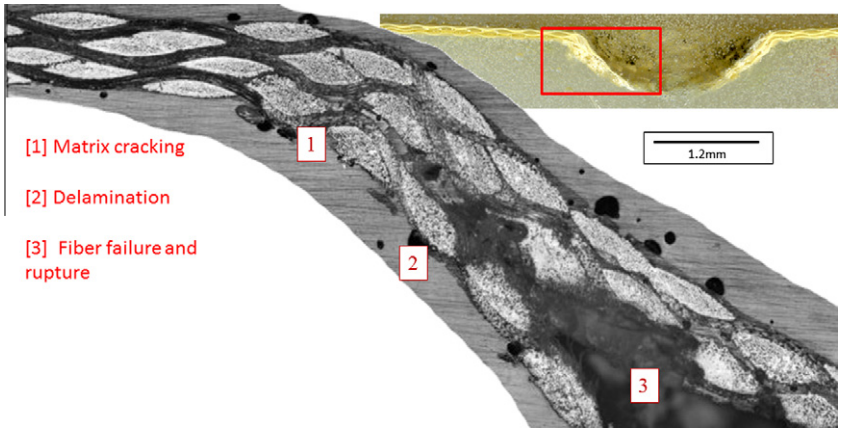

Fig. 11. Cross-section of the Epoxy-3K plate just under the impactor side.

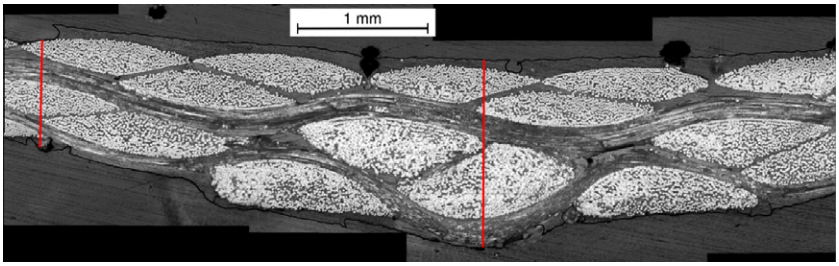

Fig. 12. Cross-section of the Epoxy-NS-3K plate.

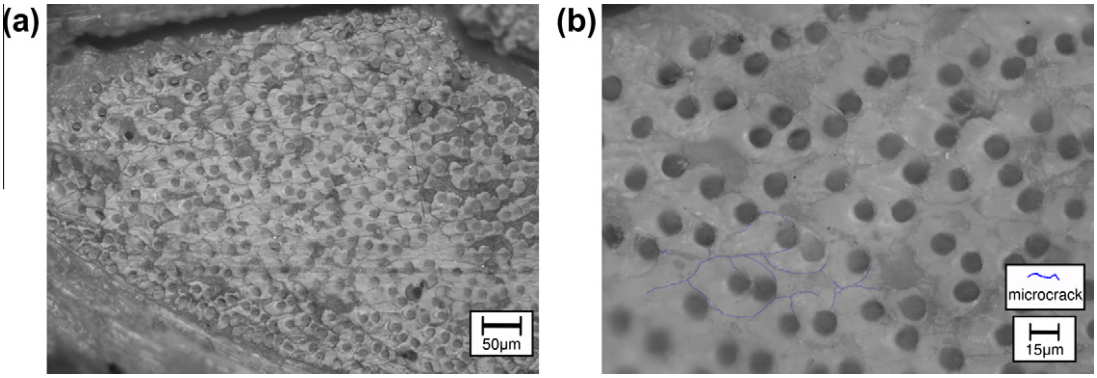

Fig. 13. Micrographs showing the significant rate of micro crack in the yarn located in the last ply of the composite structure.

concentrated since this yarn geometry is sharply disrupted (in zone 1, Fig. 11) where the curvature radius of the structure (imposed by the projectile) is most significant. The geometry of the yarn section changes drastically, and its area also increases significantly due to matrix cracks initiated between the fibers. A gap can be detected between plies' interface (zone 2, Fig. 11) revealing then the initiation of delamination which appears between the layers of the composite sheet. Finally, fiber breakages can be noticed close to the impact point (zone 3, Fig. 11).

3.2.2.2. Microscopic observations on Epoxy-NS-3K. Microscopic observations Epoxy-NS-3K (Fig. 12) revealed an important increase in thickness structure in the impact zone, from 0.80 mm (far to the impact point) to 1.45 mm at the impact point. Yarns in the second and last plies of the composite are strongly damaged; the geometry of their cross-section is severely modified and their areas increase significantly. This observation suggests that damage processes occur mainly in the yarn and are intra-yarn matrix cracks.

More accurate observations (Fig. 13) reveal a high density of micro matrix cracks between fibers into the yarn. These are mainly responsible for the dissipated energy. Moreover, a delamination zone over 7.68 mm is revealed between the bottom layer and the middle layer. These two phenomena, micro cracks and delamination, are responsible for the dissipation of the impact energy.

3.3. Influence of phisico-chemical parameters

3.3.1. Definition of criteria

In order to compare the influence of parameters, two criteria are defined (Fig. 14).

The first one is defined as the energy until the initiation of the perforation. This one is computed as the integral of the force–displacement curve from 0 mm and the displacement corresponding to the beginning of fiber rupture. The displacement corresponding to the fiber rupture can be determined from observation of the high-speed video of the back face of the plate.

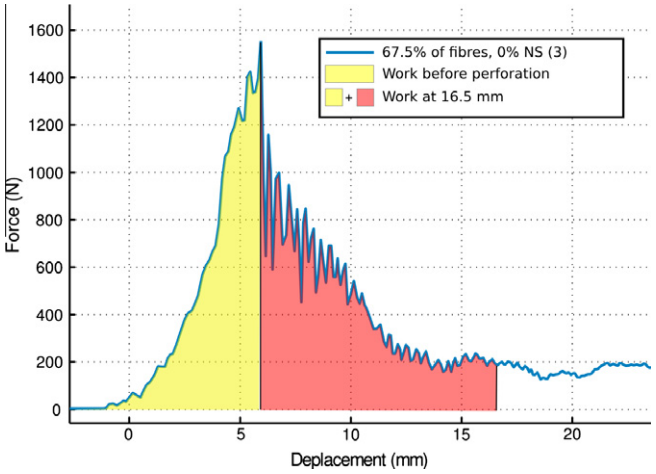

Fig. 14. Cross-section of the Epoxy-NS-3K plate.

Moreover, the observation of images and force curve revealed that the beginning of fiber breakage occurs just after maximum force. Finally, we defined the first criterion as the integral of the force–displacement curve between 0 mm and the displacement corresponding to maximum force. This energy represents the elastic energy of the plate, the energy dissipated by matrix damage, the energy dissipated by friction and energy dissipated by wave propagation in the experimental devices. A composite plate resist to perforation as many as this criterion have an important value. A ranking regarding perforation resistance can be performed with this criterion.

The second criterion is defined as the energy from 0 mm until a displacement of 16.5 mm. The value of 16.5 mm has been chosen arbitrarily and corresponds to a value where the perforation and penetration of the impactor systematically happen. This energy represents the residual elastic energy of the plate, the energy

dissipated by matrix damage, the energy dissipated by fiber breakage, the energy dissipated by friction, and the energy dissipated by wave propagation in the experimental devices. A ranking regarding energy dissipated by plate perforation can be performed with this criterion.

These two criteria help us to make a comparison; however, all plates have a different weight and thickness. Indeed, all plates have three layers and a different fiber-weight ratio. As all plates are the same area, that means the same weight of fiber but different weight of matrix, and therefore different thickness. So, we have to keep in mind that the difference of thickness induces a different bending rigidity and a different duration of contact time, and thus different test conditions. Specific values of the two previous criteria have to be introduced, and are defined as the criterion value divided by the surface density.

3.3.2. Comparison of criteria

The expected increase in energy to perforate and the energy dissipated by the perforation with the decreasing fiber weight ratio is verified only for the Epoxy-3K (Fig. 15). That is surprising, because, as previously explained; a weak fiber weight ratio means the same amount of fibers but a higher amount of matrix, so more material. A possible explanation for the Epoxy-NS-3K is that for the thick composite plate the damage area is smaller than for the thin plate due to localization.

3.3.3. Comparison of specific criteria

Specific values of criteria, defined at the end of Section 3.3.1, are presented in Fig. 16. First of all, the increase of specific values vs. the fiber weight ratio are verified for all composites whatever the composition. At this point of analysis, the matrix resin previously degassing and not previously degassing shows a difference that can be neglected compared to the dispersion of the measuring incertitude even if there is a little increase of dissipated energy for a plate with 38% of fiber.

Now, if we look at the evolution of both criteria fixing the percentage of Nanostrength, an important increase is noticed. This could be easily explained by the higher specific properties of Kevlar fibers than epoxy matrix. However, for 10% of Nanostrength, from 35% to 68% of the fiber weight ratio, the increase is about 275% for the energy to perforate and 150% for the energy dissipated by perforation. Whereas, the increase is about only 35% for the energy to perforate and 68% for the energy dissipated by the perforation for the same range of fiber weight ratio variation. Those significant

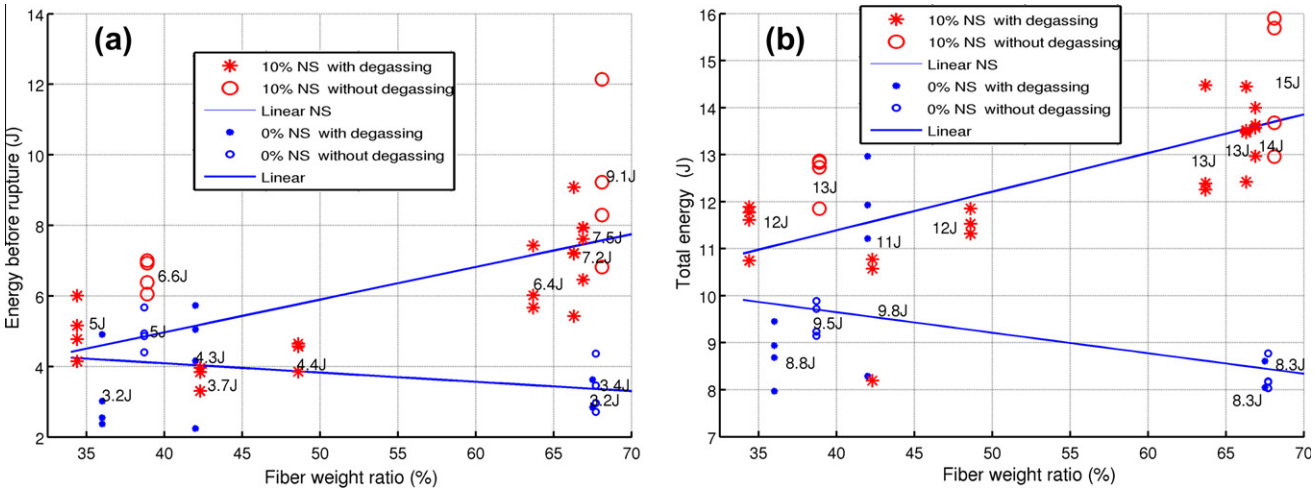

Fig. 15. Evolution of the two criteria vs. fiber weight ratio, for impact with a 1 m height.

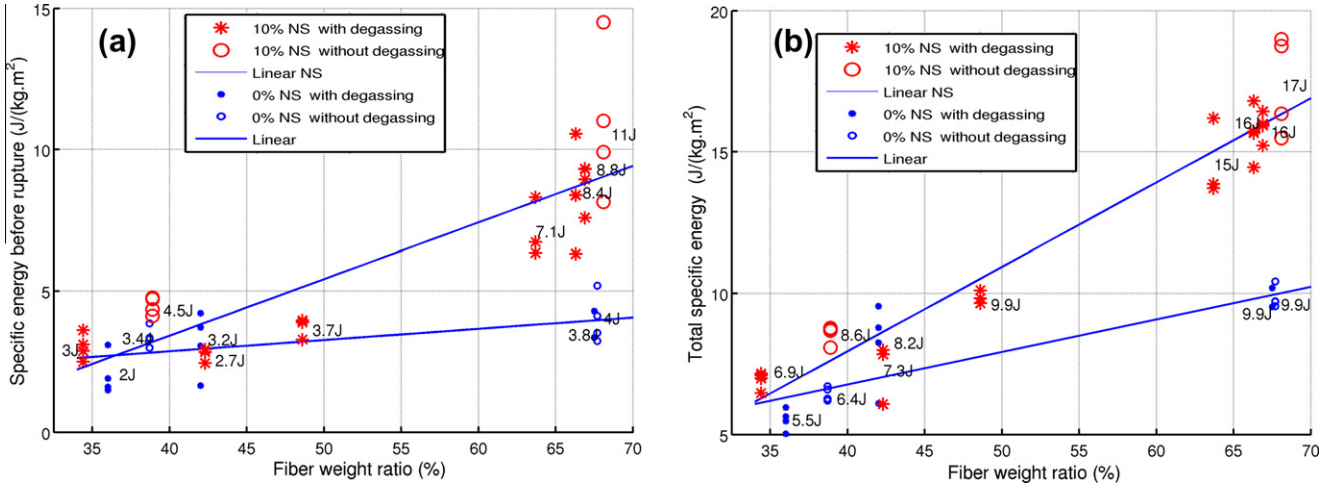

Fig. 16. Evolution of the two specific criteria vs. fiber weight ratio, for impact with a 1 m height.

increased criteria, especially the first one, could be explained by three contributions induced by the addition of Nanostrength. The first contribution of Nanostrength is to increase the amount of elastic energy stoked in the plate by postponing the elastic limit (i.e. increase the contact time). Moreover, the second contribution is probably due to the important amount of energy dissipated by the matrix damage. Indeed, epoxy with Nanostrength is much more resilient than epoxy ifself; this is due to the nano-cavitation process and shear yielding. The third one is linked to the coupling of the two previous phenomena and is a larger damage area.

4. Conclusion

The objective of this research was to evaluate the dynamic response of composites based on Kevlar fibers with different types of matrix including various nanoparticles (Nanostrength). A drop weight tower was used to conduct low-velocity impact tests on the three kind of composites, and the specific boundaries of the sample were determined to reproduce similar damage patterns on the specimen similar to that observed in industrial application (helmet). The effect of these nanocharges (M22N, M42N and M52N) on the composites under low-velocity impact was firstly studied at the macroscopic level. Then M52N bock-copolymer was chosen and different percentages were tested (5% 10% and 15%). A comparison between Epoxy-3K and Epoxy-NS-3K was performed at mesoscopic scales to describe the different failure mechanisms.

The addition of elastomeric nanocharges drastically increases the strength of the composite under impact. If one can note a decrease in the macroscopic elastic stiffness, resistance to the impact is higher since any perforation cannot be detected for similar impacts. The damage was not localized in the impacted zone but was spread across a significant part of the structure. In this case, the damage phenomena consist mainly of matrix cracking.

A study on the influence of physicochemical parameters was performed owing to the definition of two criteria (energy to perforate and energy dissipated by the perforation). The fiber weight ratio has an important influence on the criteria, and Nanostength enhancement is clearly favored by a high fiber weight ratio.

To conclude about our study, the industrial context was the improvement of the design of an helmet in modifying firstly the behavior of the composite. Kevlar fibers were chosen for their good properties under dynamic conditions and this research focused on the effect of block copolymer embedded in epoxy resin. Instead of a significant effect coming from the M22 and M42, the M52N elastomeric nanocharges significantly improved the resistance of these composite structures under impact without compromising the rigidity.

References

[1] Mills NJ, Fitzgerald C, Gilchrist A, Verdejo R. Polymer foams for personal protection: cushions, shoes and helmets. Compos Sci Technol 2003;63(16):2389–400.
[2] Viot P. Polymer foams to optimize passive safety structures in helmets. Int J Crashworthiness 2007;12(03):299–310.
[3] DiLandro L, Sala G, Olivieri D. Deformation mechanisms and energy absorption of polystyrene foams for protective helmets. Polym Test 2002;21:217–28.
[4] Naik N, Shrirao P, Reddy B. Ballistic impact behaviour of woven fabric composites. Formulat Int J Impact Eng 2006;32:1521–52.
[5] Bacigalupo L, Pearson R. The use of triblock copolymers to toughen epoxy resins. In: 33rd Annual Meeting Adhesion Society in Daytona, Florida, 2010. p. 147.
[6] Barsotti R. Nanostrength block copolymers for epoxy toughening. In: Proceeding and presentation, ANTEC (SPE conference), Chicago, IL; June 22–24, 2009.
[7] Barsotti R, Chen J, Alu A. Nanostrength block copolymers for wind energy. In: Procedings and presentation, materials challenges in alternative and renewable energies, Cocoa Beach, FL; February 21, 2010.
[8] Ávila AF, Carvalho MGR, Dias EC, daCruz DT. Nano-structured sandwich composites response to low-velocity impact. Compos Struct 2010;92:745–51.
[9] Hussain S, Roy R, Pal A. Incorporation of silver nanoparticles in DLC matrix and surface plasmon resonance effect. Mater Chem Phys 2006;99:375–81.
[10] Serrano E, Gerard P, Lortie F, Pascault JP, Portinha D. Nanostructuration of unsaturated polyester by all-acrylic block copolymers. 1-Use of high-molecular-weight block copolymers. Macromol Mater Eng 2008;293:820–7.
[11] Alcock B, Cabrera N, Barkoula N-M, Peijs T. Compos Sci Technol 2006;66: 1724–37.
[12] Morais Wd, Monteiro SN, d'Almeida J. Effect of the laminate thickness on the composite strength to repeated low energy impacts. Compos Struct 2005;70:223–8.
[13] Defence standard 05–102 military aircrew helmet impact standard. Technical Rapport, Ministry of defence; 2006.
[14] Fu-Kuo Chang, Hyung Yun Choi, Syh-Tsang Jeng. Study on impact damage in laminated composites. Mech Mater 1990;10(1–2):83–95.
[15] Ballère L, Viot P, Lataillade JL, Guillaumat L, Cloutet S. Damage tolerance of impacted curved panels. Int J Impact Eng 2009;36:243–53.
[16] Sevkat E, Liaw B, Delale F, Raju BB. Drop-weight impact of plain-woven hybrid glass-graphite/toughened epoxy composites. Compos Part A: Appl Sci Manuf 2009;40:1090–110.
[17] Tita V, Carvalho Jd, Vandepitte D. Failure analysis of low velocity impact on thin composite laminates experimental and numerical approaches. Compos Struct 2008;83:413–28.
[18] Viot P, Ballère L, Guillaumat L, Lataillade J-L. Scale effects on the response of composite structures under impact loading. Eng Fract Mech 2008;75:2725–36.
[19] Mitrevski T, Marshall I, Thomson R, Jones R, Whittingham B. The effect of impactor shape on the impact response of composite laminates. Compos Struct 2005;67:139–48.
[20] Gustin J, Joneson A, Mahinfalah M, Stone J. Low velocity impact of combination Kevlar/carbon fiber sandwich composites. Compos Struct 2005;69:396–406.